NON-RIGID BIOMEDICAL IMAGE REGISTRATION USING GRAPH CUTS WITH A NOVEL DATA TERM

Ananda S. Chowdhury[1], Rounak Roy[1], Sumon Kr. Bose[1], Fahmi Khalifa[2], Ahmed Elnakib[2], Ayman El-Baz[2]
{aschowdhury@etce.jdvu.ac.in, (rounakroy.me, sumon.bose30)@gmail.com, (fakhal01, aaelna02, aselba01)@louisville.edu}

[1]Department of Electronics and Telecommunication Engineering
Jadavpur University, Kolkata – 700032, India.

[2]BioImaging Laboratory, Bioengineering Department
University of Louisville, Louisville, KY -40292, USA.

ABSTRACT

Problem of non-rigid registration has become very important in the area of biomedical imaging. A non-rigid registration problem is modeled as an optimization problem and is solved using graph cuts and MRFs in recent years. In this paper, we have improved the graph cuts-based solution to non-rigid registration with a novel data term. The proposed data term has several advantages. Firstly, displacement labels can be directly assigned from this data term. Secondly, our data term imposes stricter penalty for intensity mismatches and hence yields higher registration accuracy. Finally, this data term can efficiently handle the dissimilarities in the intensity patterns between the floating and the reference images which may also arise due to some changes in illumination in addition to motion. We show the effectiveness of the proposed method on MRI images of brain and light microscopy images of retina. Experimental results indicate the superiority of our technique over some well-known non-rigid registration algorithms.

Index Terms— Non-rigid registration, graph cuts, data term, brain MRI, retinal images.

1. INTRODUCTION

Non-rigid image registration poses a great challenge due to high degree of freedom, smoothness requirements, and difficulties to model the physical relationships between the target and reference images [1]. Some biomedical imaging problems which require non-rigid registration are deformation field recovery during surgery, motion correction, alignment of images obtained at different times and/or with different imaging parameters, and formation of composite functional maps [2]. Markov random fields (MRFs) and graph cuts are applied in recent years to solve the non-rigid registration problem [3-4]. So and Chung have improved the graph cuts-based non-rigid registration in [4] with mutual information as a measure of similarity between the intensity distributions in the floating and the reference image [5]. Assignment of displacement labels in [5] is improved in the present work with the introduction of a novel data term. The data term uses the sum of absolute differences (SAD) of the intensities in the floating and the reference images [4] as an argument of an exponential function. Firstly, displacement labels in the floating image can be directly assigned from our data term. Secondly, strict penalties for large intensity differences between the reference image and the floating image can be also imposed using this term. Furthermore, the work described in [4-5] cannot properly tackle situations where change in intensity between the reference and the floating images is caused by change in illumination in addition to the non-rigid motion. We also explicitly address this problem with our novel data term.

To demonstrate the effectiveness of our proposed method, we discuss two different biomedical applications in this paper. The first application deals with non-rigid registration of brain MRI. Non-rigid registration plays a vital role in computational neuroanatomy by helping in the detection of abnormalities like schizophrenia [6]. We show our results on MRI images of brain downloaded from Brainweb [7]. The second application is on non-rigid registration of retinal images, which is extremely important for diabetic patients [8]. In a recent paper, Zheng et al. [9] discussed registration of retinal images using salient feature regions. This method requires separate steps like matching of salient feature regions, followed by both local rigid transformation and higher-order global transformation. In contrast, we apply one-step improved graph cut method for non-rigid registration of multi-temporal fundus images obtained using light microscopy from the Kentucky Lions Eye Center. Since the main focus of this work is to show improvement in the accuracy of non-rigid registration of biomedical images in a graph cut-based framework, we compare our method with the technique described in [5]. In addition, we also show comparisons with the well-known Demons algorithm used for non-rigid registration [10].

2. METHODS

The task of image registration is to find an optimal transformation, T^*, which spatially matches a floating image, I_f, to the reference image, I_r, based on some measure of intensity dissimilarity $C(I_r, T(I_f))$. Here, we follow the notations used in [4-5]. A registration problem can be mathematically defined as:

$$T^* = \arg\min_T C(I_r, T(I_f)) \quad (1)$$

where $T(I_f)$ denotes the transformed floating image. A regularization term is often added to Eq. (1) to ensure smooth transformations. Thus, we can write:

$$T^* = \arg\min_T C(I_r, T(I_f)) + \lambda S(T) \quad (2)$$

The term $S(T)$ in Eq. (2) is called the smoothness penalty and λ is a constant denoting the amount of penalty. In the case of non-rigid transformation, the pixels in the floating image can move more freely. Therefore, a deformation vector field, $\boldsymbol{D}$, is used to represent the transformation T. So, Eq. (2) can be written as:

$$D^* = \arg\min_D C(I_r, D(I_f)) + \lambda S(D) \quad (3)$$

In [4], SAD is directly used as a measure of intensity dissimilarity. Mutual information (MI) is proposed in [5] as a better alternative. There exist several problems with these choices for the data term. Firstly, displacement labels to the pixels in the floating image cannot be directly assigned from the above dissimilarity measures. Secondly, this way of choosing labels often fails to impose strict penalty in the data term for intensity mismatches. Thirdly, change in illumination between the floating and the reference image pair cannot be properly handled. Retinal image pair in figures 4(a) and 4(b) is a point in the case. In addition to motion, change of illumination (reference image is brighter than the floating image) is prominent in this pair.

We first show how using a novel function, the first two goals can be achieved. Use of exponential functions for capturing intensity difference between pixels can be found in [11]. The proposed function for this problem is given below:

$$C(I_r, D(I_f)) = \left\lfloor \exp\left(\sum_{x \in X} \left\| I_r - D(I_f) \right\|\right) \right\rfloor \quad (4)$$

In Eq. (4), x denotes a pixel in the floating images X. Low displacement labels, which indicate more probable motions, need to be assigned to the pixels in the floating image where the intensity differences with the pixels in the reference image are small and vice-versa. Firstly, using Eq. (4), we can directly assign the labels from the corresponding values of C. Secondly, the exponential function enforces strict penalty by assigning low labels in the data term to pixels in the floating image having small intensity difference with pixels in the reference image. The floor function is used to ensure integer labels. Since we want to assign lower labels (l) for better matches and $\forall l, \lfloor l \rfloor \leq \lceil l \rceil$, a floor function is a better choice over a ceiling function. Table 1 illustrates the above concepts.

Table 1. Assignment of Labels (from Eq. (4))

$\sum_{x \in X} \left\| I_r - D(I_f) \right\|$	C(I_r, D(I_f))	Label
0	1	1
1	2	2
2	8	8
3	20	20

When $\sum_{x \in X} \left\| I_r - D(I_f) \right\|$ exceeds 3, we still assign the corresponding label to be 20. We restrict correspondences between pixels in the floating and reference images by imposing strict limits to intensity differences between them. Hence, this type of label assignment increases the registration accuracy. Note that change in illumination between two images essentially causes a shift in their intensity patterns. Hence, in case of image pairs with considerable change of illumination, only large labels will be assigned even if the change in intensity due to motion is small. As a result of this incorrect label assignment, registration accuracy gets adversely affected. We modify equation (4) by incorporating a term to capture the changes in illumination between a floating and a reference image in the following manner:

$$C(I_r, D(I_f)) = \left\lfloor \exp\left(\sum_{x \in X} \left\| I_r - D(I_f) \right\| - \partial(I_r, D(I_f))\right) \right\rfloor \quad (5a)$$

where $\partial(I_r, D(I_f)) = \min\left(\sum_{x \in X} \left\| I_r - D(I_f) \right\|\right)$ (5b)

Minimum SAD in equation (5b) for each pixel in the reference image is calculated over its local neighborhood, and is used to establish better correspondence between the reference and the floating images. Using equations (5a) and (5b), we reduce the difference in intensity between the floating and the reference images caused by change of illumination. So, more accurate labels can be assigned and better registration accuracy can be achieved. The smoothness penalty is imposed based on the concept of label consistency using MRF [11] and is given by:

$$S(D) = \sum_{x \in X, y \in N(x)} \left\| D(x) - D(y) \right\| \quad (6)$$

where $N(x)$ denotes the neighborhood of the pixel x. The energy function E_f of the graph cuts-based optimization is given by [11]:

$$E_f = \sum_{p \in P} D_p(f_p) + \sum_{p \in P, q \in N(p)} V_{pq}(f_p, f_q) \quad (7)$$

where D_p is the data term, V_{pq} is the smoothness term and $f_p(f_q)$ denotes the intensity of the pixel $p(q)$. The optimal transformation ($\boldsymbol{D}^*$) for non-rigid registration in Eq. (3) is similar to the graph cuts-based energy function (E_f) in Eq. (7). Graph cuts with α–expansion [12] is employed in the present problem to obtain optimal transformation through the assignment of multiple displacement labels.

We directly apply the above equations for registration of brain images. For the colored retinal images, we treat red (R), green (G) and blue (B) components separately [13]. So,

three optimal transformations D_R^*, D_G^* and D_B^* for the R, G and B components are obtained. Three separately registered images using D_R^*, D_G^* and D_B^* are then generated. Finally, ImageJ [14] is employed to obtain the composite non-rigidly registered image from these three components.

3. EXPERIMENTAL RESULTS

The proposed approach has been tested on 5 sets of brain MR images and 5 sets of retinal images, each of size 256 x 256 pixels. Brain MRI data are downloaded from the Brainweb [7]. The retinal images are multi-temporal colored images, captured at different times by using a ZEISS FF 450plus IR Fundus Camera with VISUPAC/System 451, which is connected to a JVC digital camera. The images were taken at the same visit or at different dates from the patients at the Kentucky Lions Eye Center. While measuring registration accuracy, entire image is considered in both the applications. We choose (mean ± standard deviation.) of the absolute intensity differences as the measure of the registration accuracy [4-5]. We use GCoptimization software [11-12] to implement our method. A first-order neighborhood with 8 neighbors is chosen. Following [4-5], we take $\lambda = 0.05 \times 255$ and select displacement label of a pixel from 31 x 31 i.e., {0, ±1, ±2, …, ±15}x{0, ±1, ±2, …, ±15}) window. In Tables 2 and 3, we respectively show the registration accuracies obtained using [10], [5] and our method on brain images and retinal images.

Table 2. Registration Accuracy for the Brainweb images

Dataset	Demons [10]	Graph Cut with Mutual Information [5]	Proposed Method
1	0.03 ± 0.17	2.9×10^{-4} ± 0.06	4.58×10^{-5} ± 0.01
2	2.69 ± 3.32	0.12 ± 3.01	0.09 ± 0.04
3	1.17 ± 2.18	0.07 ± 2.60	0.01 ± 0.05
4	1.62 ± 2.87	0.19 ± 4.14	0.01 ± 0.08
5	7.56 ± 5.88	1.49 ± 6.36	0.17 ± 1.90

Table 3. Registration Accuracy for the retinal images

Dataset	Demons [10]	Graph Cut with Mutual Information [5]	Proposed Method
1	6.88 ± 0.87	1.79 ± 1.63	0.71 ± 0.31
2	3.08 ± 4.33	1.32 ± 1.59	0.24 ± 0.12
3	7.40 ± 3.49	5.37 ± 3.06	3.19 ± 1.30
4	22.97 ± 6.10	18.28 ± 2.12	8.06 ± 2.23
5	15.76 ± 2.82	13.11 ± 3.05	5.90 ± 2.62

Due to space limitation, we only illustrate the registration results for 2 sets of brain images and 2 sets of retinal images. In figures 1 and 2, we respectively present the registration results on the dataset 2 and dataset 5 of Table 1. Similarly, in figures 3 and 4, we present the registration results on retinal images in dataset 2 and dataset 5 of Table 2. All the figures and tables clearly indicate that our proposed method outperforms both the non-rigid registration approaches proposed in [5] and [10]. Among the three methods, Demons performed worst. As mentioned in [5], Demons algorithm can be trapped in local minima and hence may yield incorrect results. The method described in [5] produces better results than the Demons but it performs worse than the proposed method. One reason is, unlike the proposed method, the method in [5] fails to capture the illumination changes between the floating and the reference images (please see figure 4). Another reason behind the better performance of our method is imposition of stricter penalty for intensity dissimilarity as compared to [5]. Average execution times for registering a brain image and a retinal image are 2 min and 6 min respectively for our method and [5] and 1.5 min and 4.5 min respectively for [10] on a typical desktop with Intel(R) Core(TM)2 Duo processor with a speed of 2.8 GHz and 2 GB of memory.

4. CONCLUSION AND FUTURE SCOPE

In this paper, we propose an improved data term for the non-rigid biomedical image registration problem, modeled as a global optimization problem and solved using graph cuts. The novel function used for obtaining the data term imposes stricter penalty for intensity mismatch between the floating and reference images caused by motion and any possible change of illumination. We qualitatively and quantitatively demonstrated the effectiveness of the proposed method on two different applications, namely, the brain MRI and the light microscopic retinal fundus images.

In future, we plan to further improve the registration accuracy by incorporating higher order terms in the energy function [15]. Another direction of future research will be to dynamically fix the window size for handling different amount of motion. We also plan to undertake a more in-depth validation of our method by applying it on large and more diverse datasets.

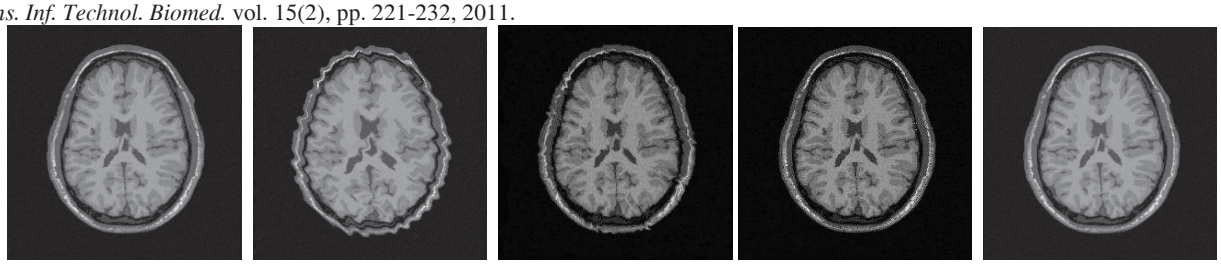
REFERENCES

[1] D. Rueckert, "Non-rigid registration: Techniques and applications," in *Medical Image Registration, CRC Press*, 2001.

[2] W R Crum, T Hartkens, and D L G Hill, "Non-rigid image registration: theory and practice," *British J. Radiol.*, vol. 77, S140-S153, 2004.

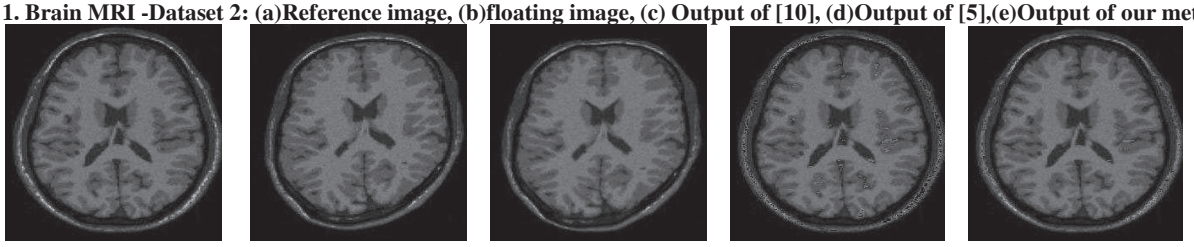
[3] B. Glocker, N. Komodakis, G. Tziritas, N. Navab, N. Paragios, "Dense image registration through MRFs and efficient linear programming," *Med. Image Anal.*, vol. 12(6), pp. 731-41, 2008.

[4] T. W. H. Tang and A. C. S. Chung, "Non-rigid image registration using graph-cuts," *MICCAI LNCS*, vol. 4791, pp. 916–924, 2007.
[5] R.W.K. So and A.C.S. Chung, "Non-rigid Image Registration By Using Graph Cuts With Mutual Information," *IEEE ICIP*, pp. 4429-4432, 2010.
[6] D. Schwarz, T. Kasparek, I. Provaznik, and J. Jarkovsky, "A Deformable Registration Method for Automated Morphometry of MRI Brain Images in Neuropsychiatric Research," *IEEE Trans. Med. Imag.* vol. 26 (4), pp. 452-461, 2001.
[7] B. Aubert-Broche, A. Evans et al, "A new improved version of the realistic digital brain phantom," *NeuroImage*, vol. 32 (1), pp. 138–145, 2006.
[8] D. Usher, M. Dumskyj, M. Himaga, T. H. Williamson, S. Nussey, and J. Boyce, "Automated detection of diabetic retinopathy in digital retinal images: a tool for diabetic retinopathy screening," *Diabetic Medicine*, vol. 21, pp. 84-90, 2003.
[9] J. Zheng, J. Tian, K. Deng, X. Dai, X. Zhang, M. Xu, "Salient feature region: a new method for retinal image registration, " *IEEE Trans. Inf. Technol. Biomed.* vol. 15(2), pp. 221-232, 2011.
[10] J. Thirion, "Image matching as a diffusion process: an analogy with maxwell's demons," *Med. Image Analysis*, vol. 2(3), pp. 243–260, 1998.
[11] Y. Boykov, O. Veksler, R. Zabih, "Fast approximate energy minimization via graph cuts," *IEEE Trans. Pattern. Anal. Mach. Intel.* vol. 23(11), 1222–1239, 2001.
[12]V. Kolmogorov and R. Zabih, "What Energy Functions can be Minimized via Graph Cuts?," *IEEE Trans. Pattern. Anal. Mach. Intel.* vol. 26(2), 147–159, 2004.
[13] Lucac R. and K. Plataniotis, *Color Image Processing: Methods and Applications*, CRC Press, Florida, USA, 2006.
[14] W.S. Rasband, ImageJ, U. S. National Institutes of Health, Bethesda, Maryland, USA, http://imagej.nih.gov/ij/, 1997-2011.
[15] P. Kohli, L. Ladicky and P.H.S. Torr, "Robust Higher Order Potentials for Enforcing Label Consistency," *Int. J. Computer Vis.,* vol. 82, 302-324, 2009.



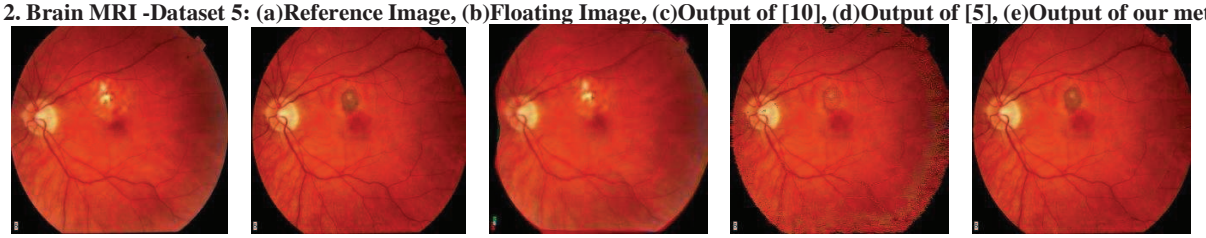
(a) (b) (c) (d) (e)

Fig. 1. Brain MRI -Dataset 2: (a)Reference image, (b)floating image, (c) Output of [10], (d)Output of [5],(e)Output of our method



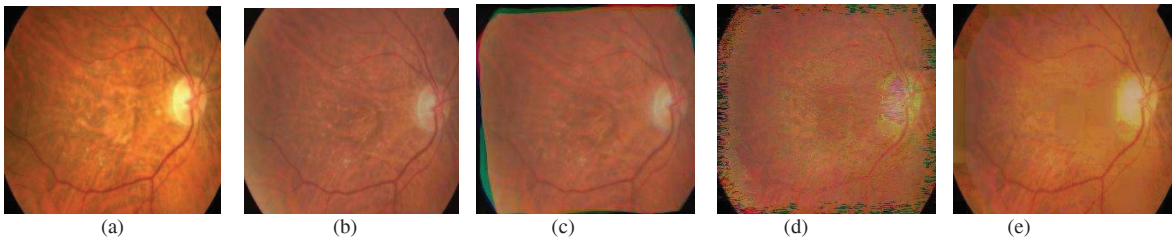
(a) (b) (c) (d) (e)

Fig. 2. Brain MRI -Dataset 5: (a)Reference Image, (b)Floating Image, (c)Output of [10], (d)Output of [5], (e)Output of our method



(a) (b) (c) (d) (e)

Fig. 3. Retinal images-Dataset 2:(a)Reference Image, (b)Floating Image, (c)Output of [10], (d)Output of [5], (e)Output of our method



(a) (b) (c) (d) (e)

Fig. 4. Retinal images -Dataset 5:(a)Reference Image, (b)Floating Image, (c)Output of [10], (d)Output of [5], (e)Output of our method